CrossMark
←click for updates

Repair of a Mutation Disrupting the Guinea Pig Cytomegalovirus Pentameric Complex Acquired during Fibroblast Passage Restores Pathogenesis in Immune-Suppressed Guinea Pigs and in the Context of Congenital Infection

Michael A. McVoy,[a] Jian Ben Wang,[a] Dirk P. Dittmer,[b] Craig J. Bierle,[c] Elizabeth C. Swanson,[c] Claudia Fernández-Alarcón,[c] Nelmary Hernandez-Alvarado,[c] Jason C. Zabeli,[c] Mark R. Schleiss[c]

Department of Pediatrics, Virginia Commonwealth University School of Medicine, Richmond, Virginia, USA[a]; Department of Microbiology and Immunology, University of North Carolina at Chapel Hill, Chapel Hill, North Carolina, USA[b]; Center for Infectious Diseases and Microbiology Translational Research, Division of Pediatric Infectious Diseases, Minneapolis, Minnesota, USA[c]

ABSTRACT

Guinea pig cytomegalovirus (GPCMV) provides a valuable model for congenital cytomegalovirus transmission. Salivary gland (SG)-passaged stocks of GPCMV are pathogenic, while tissue culture (TC) passage in fibroblasts results in attenuation. Non-pathogenic TC-derived virus N13R10 (cloned as a bacterial artificial chromosome [BAC]) has a 4-bp deletion that disrupts *GP129*, which encodes a subunit of the GPCMV pentameric complex (PC) believed to govern viral entry into select cell types, and *GP130*, an overlapping open reading frame (ORF) of unknown function. To determine if this deletion contributes to attenuation of N13R10, markerless gene transfer in *Escherichia coli* was used to construct virus r129, a variant of N13R10 in which the 4-bp deletion is repaired. Virions from r129 were found to contain GP129 as well as two other PC subunit proteins, GP131 and GP133, whereas these three PC subunits were absent from N13R10 virions. Replication of r129 in fibroblasts appeared unaltered compared to that of N13R10. However, following experimental challenge of immunocompromised guinea pigs, r129 induced significant weight loss, longer duration of viremia, and dramatically higher (up to 1.5×10^6-fold) viral loads in blood and end organs compared to N13R10. In pregnant guinea pigs, challenge with doses of r129 virus of $\geq 5 \times 10^6$ PFU resulted in levels of maternal viremia, congenital transmission, pup viral loads, intrauterine growth restriction, and pup mortality comparable to that induced by pathogenic SG virus, although higher doses of r129 were required. These results suggest that the *GP129-GP130* mutation is a significant contributor to attenuation of N13R10, likely by abrogating expression of a functional PC.

IMPORTANCE

Tissue culture adaptation of cytomegaloviruses rapidly selects for mutations, deletions, and rearrangements in the genome, particularly for viruses passaged in fibroblast cells. Some of these mutations are focused in the region of the genome encoding components of the pentameric complex (PC), in particular homologs of human cytomegalovirus (HCMV) proteins UL128, UL130, and UL131A. These mutations can attenuate the course of infection when the virus is reintroduced into animals for vaccine and pathogenesis studies. This study demonstrates that a deletion that arose during the process of tissue culture passage can be repaired, with subsequent restoration of pathogenicity, using BAC-based mutagenesis. Restoration of pathogenicity by repair of a frameshift mutation in GPCMV gene *GP129* using this approach provides a valuable genetic platform for future studies using the guinea pig model of congenital CMV infection.

Infection with human cytomegalovirus (HCMV) is a leading cause of disability in newborns, and development of an effective vaccine is a major public health priority (1, 2). Preclinical modeling of vaccines against congenital infection must rely on the study of species-specific CMVs, since HCMV will not infect nonhuman cells (3, 4). The study of guinea pig cytomegalovirus (GPCMV) is particularly valuable, since this virus will cross the placenta and infect pups *in utero*, leading to congenital transmission (5). Thus, the GPCMV model has been utilized to examine a variety of subunit vaccine and antiviral therapy strategies relevant to human health (6–8).

Prior studies reported the successful cloning of the genome of a tissue culture-attenuated variant of GPCMV strain 22122 as a bacterial artificial chromosome (BAC) designated N13R10 (9). Although virus derived from N13R10 grows like wild-type GPCMV in cell culture, it was highly attenuated *in vivo* compared to pathogenic salivary gland (SG)-adapted virus. Similar work

from other groups had previously demonstrated that a GPCMV lacking a 1.6-kb region of the viral genome was attenuated *in vivo* (10). Attenuation of N13R10 was observed in studies in which a high dose (10^8 PFU) was administered to young female guinea

pigs. This dose of virus produced transient viremia and impaired weight gain, but did not cause mortality (11). A dose of 5×10^5 PFU administered to pregnant animals caused congenital infections in 60% of live-born pups but relatively low (17%) pup mortality (12). In contrast, challenge of pregnant guinea pigs with substantially lower doses of virulent, SG-adapted virus is highly pathogenic *in vivo*. A dose as low as 1.7×10^5 PFU results in 60% dam mortality, and a dose of as little as 3.5×10^3 PFU can produce up to 80% pup mortality (13). Based on these comparisons to SG virus, adult guinea pigs tolerate a 5,880-fold-higher dose of N13R10 without significant illness or mortality, while a 140-fold-higher dose of N13R10 during pregnancy produces lower rates of fetal transmission and pup loss (11, 12). The molecular basis for the attenuation of N13R10 is uncertain, but DNA sequence comparisons of the SG virus and N13R10 genomes identified only two differences resulting in alteration of annotated protein coding sequences: (i) a 4-bp deletion that disrupts overlapping genes *GP129* and *GP130* and (ii) a missense mutation in *GP130* 3′ of the 4-bp deletion/frameshift (14, 15).

Work published by several investigators has elucidated that *GP129*, *GP131*, and *GP133* encode three subunits of a protein complex analogous to the pentameric complex (PC) that mediates entry of HCMV into monocytes and epithelial/endothelial cells (10, 16–18). Deletion of this locus or disruption of individual genes in GPCMV has previously been hypothesized to contribute to attenuation (10). The absence of other deletions or mutations impacting annotated coding sequences in the N13R10 genome (14) strengthened this hypothesis and prompted us to examine whether loss of GP129 accounted for attenuation of N13R10 virus. To test this hypothesis, we repaired the N13R10 *GP129-GP130* region to match that of the SG stock of GPCMV and then evaluated the mutant parental virus (N13R10) and repaired virus (r129) for growth properties and gene expression *in vitro* and for virulence *in vivo*. The r129 virus was strikingly more virulent than N13R10, confirming that mutations impacting *GP129* and *GP130* contribute to the attenuation of N13R10. The increased pathogenicity of r129, which can be manipulated using BAC genetics, will greatly facilitate vaccine and pathogenesis studies in the GPCMV model of congenital infection.

MATERIALS AND METHODS

Virus and cells. Cell culture propagation of virus was carried out in guinea pig lung fibroblast cells (GPL cells [ATCC CCL158]) maintained in F-12 medium supplemented with 10% fetal calf serum (FCS [Fisher Scientific]), 10,000 IU/liter penicillin, 10 mg/liter streptomycin (Gibco-BRL), and 0.075% NaHCO$_3$ (Gibco-BRL). Growth curves and viral titers were determined as described previously (9).

Construction of N13R10-r129 BAC and reconstitution of viruses N13R10 and r129. BAC N13R10 contains the complete GPCMV strain 22122 genome (9), with a deletion that disrupts open reading frames (ORFs) *GP129* and *GP130*. BAC N13R10-r129 was constructed using a two-step galactokinase-mediated recombineering approach (19). In the first step, nucleotides (nt) 205537 to 206226 of BAC N13R10, comprising exon 3 of *GP129*, as annotated in GenBank accession no. KM384022 (14), were deleted and subsequently replaced with a *galK* cassette encoding galactokinase. To generate this deletion construct, oligonucleotides GP129-galk-FW (CGCCGATTCTATCGCTTGCCTGCTAATAAATTG GAACTGGACGTGATAAAACGACTCACTATAGGGCGAATTGG) and GP129-galk-RV (TACTTCCCGTTACCATCGACTGAATAAAACTCGC TACCGCAGACGTCCACGCTATGACCATGATTACGCCAAGC) were synthesized to contain 50 bp of GPCMV sequences (underlined) flanking the region to be deleted followed by 24-bp sequences complementary to

plasmid p*galK* encoding the *galK* cassette (19). Using GP129-galk-FW and GP129-galk-RV as primers and p*galK* DNA as the template, a 1.5-kb PCR product was produced containing the *galK* cassette flanked by 50-bp GPCMV targeting homologies. The product was purified using a Qiagen PCR purification kit, restricted with DpnI to digest any residual p*galK* DNA, and then phenol-chloroform extracted and ethanol precipitated.

Heat-induced electrocompetent *Escherichia coli* strain SW102 (9) cells containing BAC N13R10 were produced as follows. Cells were incubated with shaking at 32°C in LB containing 12.5 μg/ml chloramphenicol until an optical density at 600 nm (OD$_{600}$) of 0.6 was reached. Ten milliliters of culture was then transferred to a 75-cm^2 tissue culture flask and heat induced by shaking at 42°C for exactly 15 min. The culture was chilled in a water-ice slurry for 5 min and then pelleted at 5,000 rpm at 0°C for 5 min. Cells were washed twice with ice-cold water and resuspended in ice-cold water to a final volume of 50 μl.

Heat-induced electrocompetent cells were combined with 200 ng of the PCR product described above, transferred to a prechilled 0.1-cm electroporation cuvette (Bio-Rad), and electroporated at 1.8 kV with a Bio-Rad MicroPulser set to program EC1. Electroporated cells were diluted in 1 ml LB and incubated with shaking for 1.5 h at 32°C, then washed twice in M9 salts, resuspended in 100 μl M9 salts, spread on Gal-positive selection plates (19), and incubated at 32°C.

Colonies were screened by PCR using primer galk-test3 (GCTGTCG TCATCATCAACAG) located within *galK* sequences and primer delt129-galk down (GGTTATACGTGAACACGACG) located in GPCMV sequences adjacent to the inserted *galK* cassette. BAC DNAs from colonies that produced the predicted 746-bp product were further analyzed by HindIII digestion. A clone exhibiting a novel 5.1-kb HindIII fragment relative to BAC N13R10 (data not shown) consistent with insertion of the *galK* cassette was selected and designated BAC N13R10-Δ129-galk.

In the second step, selection against galactokinase was used to replace the *galK* cassette with wild-type *GP129* exon 3 sequences. PCR using primers GP129-out FW (CTGACCAGCTTGAGAACGTA) and GP129-out RV (ATTAAGCATGGGCGACATCC) was used to generate a 1.2-kb product from DNA extracted from a pathogenic salivary gland stock of GPCMV strain 22122 (20). The product was gel purified, and 200 ng was electroporated into heat-induced electrocompetent *E. coli* strain SW102 cells containing BAC N13R10-Δ129-galk as described above. After electroporation, cells were diluted in 8 ml LB and incubated with shaking at 32°C for 4.5 h. One milliliter of culture was washed twice in M9 salts, resuspended in 100 μl M9 salts, and then spread on Gal counterselection plates (19) and incubated at 32°C.

Colonies were screened by PCR using two primer pairs: (i) GP129 up-FW (CGGCGCTAAACTCTACGTTA) and GP129 mid-RV (TGTTG CACGCGACGATCTTT) and (ii) GP129-mid FW (GACGCCACACTTT CCGAGAG) and GP129-down-RV (ATCAAGAGACGTCCGGCGGA). BAC DNAs from colonies that produced the predicted 584- and 746-bp products, respectively, were further analyzed by HindIII digestion. A clone exhibiting loss of the novel 5.1-kb fragment relative to BAC N13R10-Δ129-galk (data not shown), consistent with replacement of the *galK* cassette with wild-type *GP129* exon 3 sequences, was selected and designated BAC N13R10-r129. Direct Sanger sequencing of N13R10-r129 BAC DNA confirmed that both the 4-bp deletion and the missense mutation were repaired to match SG virus sequence. However, two apparently spontaneous mutations were detected near the C-terminal end of GP130 that resulted in R93Q and P97S substitutions in the predicted amino acid sequence of GP130. As these mutations were within the intron between exons 1 and 2 of *GP129* on the negative strand, they did not impact the *GP129* ORF coding sequences.

Viruses N13R10 and r129 were reconstituted by cotransfection of BAC DNAs N13R10 or N13R10-r129, respectively, with plasmid pCre followed by limiting dilution isolation of viruses negative for green fluorescent protein expression (BAC origin-excised) as described previously (21). Virion DNA from virus r129 was PCR amplified using primers GP129-out

FW and GP129-out RV, and the product was Sanger sequenced to confirm the absence of the 4-bp mutation.

For analysis of genome stability following serial passage of r129 virus in cell culture, a viral isolate from a positive blood culture (P0) from a cyclophosphamide-treated animal (described below) was subjected to serial passage in GPL cells on a monthly basis for 11 consecutive passages. PCR employed the primers originally described by Nozawa ([10]): primer 1.6 Kb P1 (GTAGGTACCCGCAGGTTTGC) and primer 1.6 Kb P2 (TTGATCACGGACGACGATAC). PCR products were subjected to agarose gel electrophoresis to examine for full-length and deletion variants, as described by Nozawa ([10]), using DNA extracted from serially passaged ATCC (22122 strain) virus as a comparator. PCR amplification products were sequenced by standard Sanger sequencing. Real-time quantitative PCR (qPCR) was also performed on DNA extracted from each passage using previously described primers for the $GP83$ gene ([8]) and a primer-probe set spanning a 184-bp region corresponding to the $GP133$ gene (positions 206914 through 207097 as annotated in GenBank accession no. KM384022). These primers were forward primer 5′-TATTCCGTCAATGCTCACCA-3′, reverse primer 5′-CCAACTGGCCCACTACATCT-3′ and probe CFR610-TCGAGATCATTGGACAGCTG-BHQ2. ("BHQ2" is black hole quencher 2.) The PCR was performed in a 25 μl mixture using LightCycler 480 Probes Master from Roche, as well as 0.4 μM primers, 0.1 μM probe, and 0.4 U of uracil-DNA glycosylase (UNG). PCR was performed using the LightCycler 480 real-time PCR system (Roche) under the following conditions: UNG incubation at 40°C for 10 min, with initial denaturation at 95°C for 10 min, followed by 95°C for 10 s, 56°C for 15 s, and 72°C for 10 s for a total of 45 cycles, and then a final hold step at 40°C. Data were analyzed with the LightCycler data analysis software (version 1.5; Roche) using standard curves generated with serial dilutions of BAC N13R10-r129 at known concentrations.

Animal pathogenicity studies. All animal procedures were conducted in accordance with protocols approved by the Institutional Animal Care and Use Committee at the University of Minnesota, Minneapolis. Outbred nonpregnant or timed-pregnant Hartley guinea pigs were purchased from Elm Hill Laboratories (Chelmsford, MA). Animals were assessed as GPCMV IgG seropositive or seronegative by enzyme-linked immunosorbent assay (ELISA) as previously described ([22]).

Viral challenge studies were performed with cyclophosphamide-treated immunocompromised guinea pigs as previously described ([23]). Three groups ($n = 5$/group) of nonpregnant seronegative Hartley guinea pigs were treated with 100 mg/kg cyclophosphamide by intraperitoneal injection 1 day prior to and 7 days after viral challenge. Animals were challenged with virus r129 or N13R10 or sham infected with phosphate-buffered saline (PBS). Viruses were administered subcutaneously (s.c.) at a dose of 5×10^7 PFU. Animal weights were monitored every 3 to 5 days, and blood samples were obtained on days 0, 3, 7, 14, and 21 postinoculation for viral load determination by qPCR. Two animals in the r129 group became moribund due to extreme weight loss and were sacrificed on days 21 and 24. The remaining animals were sacrificed on day 28. Liver, salivary gland, lung, and spleen samples were collected for viral load determination by qPCR.

Pregnancy status was monitored by palpation. For pregnancy/challenge studies seronegative ($n = 18$) or seropositive ($n = 6$) timed-pregnant animals were challenged s.c. at approximately 35 days of gestation with either 1×10^5 PFU of SG-GCMV or 5×10^7, 5×10^6, or 5×10^5 PFU of r129 virus. This dose range was chosen primarily to identify the optimal dose of r129 virus required for inducing pup mortality. Maternal bleeds were obtained 7 days postchallenge for qPCR. Pregnancy outcomes were monitored, and pup tissues were immediately harvested from stillborn pups at delivery or within 72 h postdelivery for live-born pups.

Western blot assays. Western blot assays were conducted using standard protocols, with virus particles purified as described previously ([15]). Virus particles from N13R10, r129, and SG virus (passaged once in GPL cells; 10 μg per lane) were separated by SDS-PAGE, transferred to nitrocellulose membranes, and probed using antibodies specific for GPCMV

proteins (Fig. 2A). GPCMV glycoprotein B (gB) was detected using murine monoclonal anti-gB antibodies IE3-21 ([3]) or 29.29. Rabbit and guinea pig antisera specific to GP129, GP131, and GP133 are described elsewhere ([15]). The guinea pig antiserum to GP129 was raised against a glutathione S-transferase (GST) fusion protein, including GP129 residues Asn$_{146}$ through Lys$_{179}$ of the GP129 ORF, and was therefore not predicted to react with any putative truncated forms of GP129 corresponding to the first 101 codons of the ORF that might be expressed in the context of the 4-bp deletion mutation. A rabbit antipeptide serum specific for GPCMV gH was generated by immunization with the synthetic peptide SGSGRR DYSEARIAEI conjugated to keyhole limpet hemocyanin (Pacific Immunology). The GP133 antiserum was used at a 1:100 dilution; antiserum to GP129, GP131, or gH, was used at a 1:200 dilution. Horseradish peroxidase (HRP)-conjugated anti-rabbit IgG secondary antibody (Cell Signaling Technologies) was used at a 1:20,000 dilution; HRP-conjugated anti-mouse and anti-guinea pig IgG (Cell Signaling Technologies) antibodies were used at 1:5,000 dilutions. Western blots were developed using the ECL Prime enhanced chemiluminescence Western blotting reagent (GE Biosciences), and autoradiography was carried out according to the manufacturer's specifications.

Real-time qPCR analysis. Viral loads were determined by qPCR as described previously ([8], [24]). Briefly, DNA was extracted from either 100 μl citrated blood (MagNA Pure LC DNA isolation kit I; Roche) or from tissues obtained at necropsy using 0.1 g of homogenized frozen samples of liver, lung, or spleen (MagNA Pure LC DNA isolation kit II; Roche). Amplification primers GP83TM_F1 (CGTCCTCCTGTCGGTCAAAC) and GP83TM_R1 (CTCCGCCTTGAACACCTGAA) were used at a final concentration of 0.4 μM, while the $GP83$ hydrolysis probe (6-carboxyfluorescein [FAM]-CGCCTGCATGACTCACGTCGA-BHQ1) was used at 0.1 μM. PCR was performed using the LightCycler 480 real-time PCR system (Roche) under the following conditions: 40°C for 10 s and 95°C for 15 min, followed by 45 amplification cycles of 95°C for 10 s, 56°C for 15 s, and 72°C for 10 s. Data were analyzed with the LightCycler data analysis software (version 1.5; Roche) using standard curves generated from known copy numbers of modified plasmid pCR 2.1 containing $GP83$ sequences ([24]). DNAemia was expressed as the total number of genome copies per milliliter of blood. The limit of detection was approximately 200 copies/ml. For the purpose of statistical comparisons, a level of 100 copies/ml was assigned to negative samples. Tissue viral loads were expressed as genome copies per milligram of tissue. The limit of detection was approximately 2 genome copies/mg tissue. For the purpose of statistical comparisons, a value of 1 copy/mg was assigned to negative samples.

Histological and IFL analyses. Liver samples were harvested from two r129-infected guinea pigs (21 and 24 days postchallenge) and one sham-infected guinea pig (day 28 postchallenge). Tissue samples were washed in ice-cold PBS, fixed with fresh 4% paraformaldehyde (PFA), and then cryoembedded in Tissue-Tek OCT compound (Sakura Finetek) and frozen in liquid nitrogen. Sections of 7 μm were air-dried and fixed in 4% PFA, stained with hematoxylin and eosin, mounted using Permount (Fisher), and examined by light microscopy. For immunofluorescence (IFL), sections were permeabilized with 0.1% Triton X-100 in PBS for 30 min at room temperature, washed three times in PBS, and then incubated in blocking buffer (10% normal goat serum) for 1 h at room temperature. Following overnight incubation at 4°C with mouse anti-GPCMV gB 29.29 monoclonal antibody (1:500), slides were washed in 0.3% Tween 20 and incubated with Alexa Fluor 488-conjugated goat anti-mouse IgG secondary antibody (1:500 [Molecular Probes]) followed by staining of cellular nuclei with DAPI (4′,6-diamidino-2-phenylindole) Fluoromount-G (Electron Microscopy Sciences, PA). For immunoenzymatic detection methods, endogenous peroxidase activity was blocked by incubating slides in 3% H_2O_2 in tap water. Slides were blocked in 2.5% horse serum for 30 min followed by incubation at 4°C with an anti-guinea pig GP83 rabbit monoclonal antibody (1:1,000). After washing in 0.3% Tween 20, slides were incubated for 1 h at room temperature with ImmPRESS reagent anti-rabbit Ig (Vector Laboratories, CA) and washed and incubated
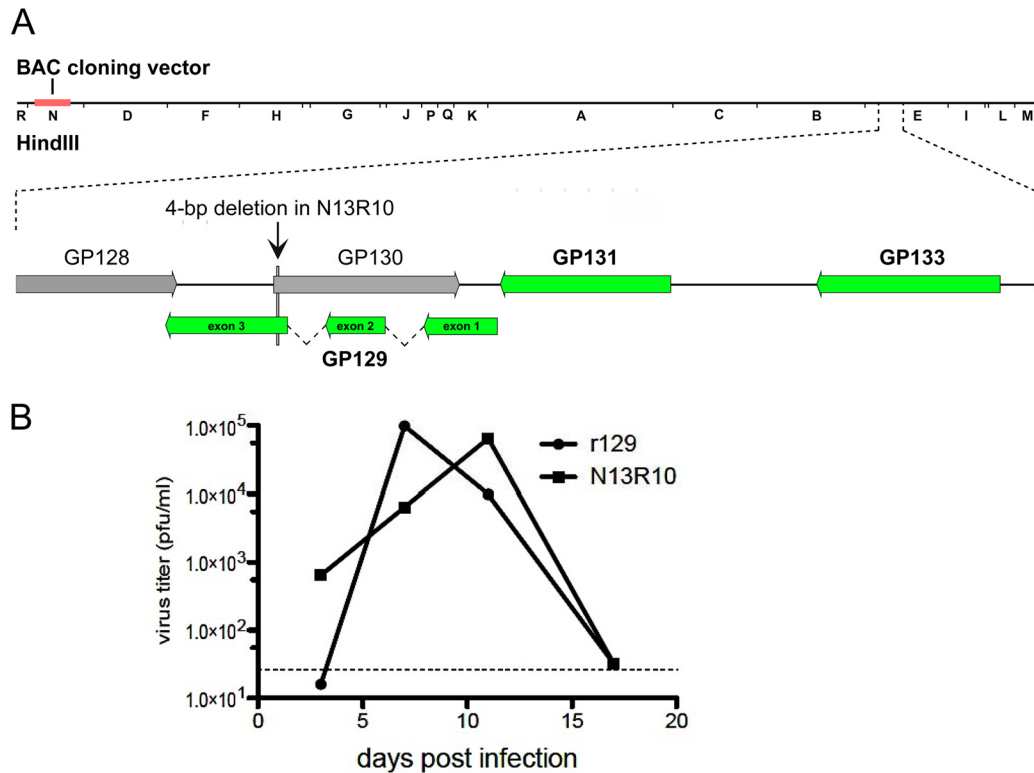
FIG 1 Structure and *in vitro* growth properties of virus r129. (A) HindIII restriction map of the GPCMV genome showing the location of BAC cloning vector sequences in N13R10. The *GP129*-to-*GP133* locus is expanded below. Genes that encode PC subunits are shown in green, while ORFs encoding uncharacterized hypothetical proteins are in gray. The location of a 4-bp deletion present in BAC N13R10 (13, 14, 17) that impacts both *GP129* exon 3 and *GP130* is shown. (B) GPL cells were infected with virus r129 or parental virus N13R10 at an MOI of 0.01, and virus titers in the culture supernatants were determined through 17 days postinfection. The dashed line indicates the limit of detection.

in ImmPACT diaminobenzidine (DAB) peroxidase (HRP) substrate solution (Vector Laboratories, CA). The slides (see Fig. 7) were counterstained with hematoxylin QS nuclear stain according to the manufacturer's instructions (Vector Laboratories).

Statistical analyses. GraphPad Prism (version 6.0) was used for statistical analyses. Parametric data included viral load measurements in blood and pup tissue and weight loss in cyclophosphamide challenge studies. These were compared using 2-way analysis of variance (ANOVA) followed by posttest Bonferroni multiple comparison.

RESULTS

Restoration of wild-type GP129-GP130 sequences in BAC N13R10. The HCMV PC is composed of glycoproteins H and L (gH and gL, respectively) complexed with UL128, UL130, and UL131A proteins. Orthologous subunits of these HCMV UL proteins form the GPCMV PC, consisting of gH, gL, GP129, GP131, and GP133, respectively (15–18). As shown in Fig. 1A, the *GP129* gene, which encodes the GP129 subunit, is comprised of three exons on the complementary (leftward direction) strand. Adjacent and also on the complementary strand are genes *GP131* and *GP133*, which encode the GP131 and GP133 proteins, respectively. Overlapping *GP129* on the opposite strand is an uncharacterized hypothetical ORF, *GP130*. As shown in Fig. 1A, a 4-bp deletion in N13R10 frameshifts *GP130* near the 5′ end and also frameshifts *GP129* near the 5′ end of exon 3 (14), thus disrupting both predicted proteins.

To ascertain if the 4-bp deletion contributes to attenuation of N13R10 virus, markerless gene transfer in *E. coli* was used to re-

place the mutant *GP129* and *GP130* sequences in N13R10 with wild-type sequences from SG virus to make virus r129 (for details, see Materials and Methods). Sequencing of r129 DNA confirmed repair of the 4-bp deletion such that *GP129* and *GP130* reading frames were restored. These genetic manipulations resulted in two spontaneous mutations that produced R93Q and P97S substitutions in the predicted amino acid sequence of GP130 but did not alter the predicted GP129 amino acid sequence, because both substitutions fell within the intron between exons 1 and 2 of GP129. In sequencing of neighboring ORFs, an incidental amino acid substitution was also noted in GP131, H131N. These sequences were stable following serial passage of virus through >10 passages in cell culture (described below). In a growth curve experiment starting with a multiplicity of infection (MOI) of 0.01, r129 replication in GPL fibroblasts was similar to that of parental virus N13R10 with respect to both kinetics and yield of infectious virus production (Fig. 1B). Thus, repair of the frameshift mutation in the GP129 sequence did not significantly impair or enhance GPCMV replication in cultured fibroblasts.

Repair of the 4-bp deletion in *GP129* and *GP130* restores virion incorporation of GP129, GP131, and GP133 proteins. In HCMV, mutations that disrupt expression of any of the three PC subunits (UL128, UL130, or UL131A) result in the generation of a virus that fails to incorporate the other two subunits into virions (25). To determine if a similar all-or-none phenomenon occurs in GPCMV, r129 and N13R10 virion particles were purified and analyzed by Western immunoblotting using monoclonal antibodies
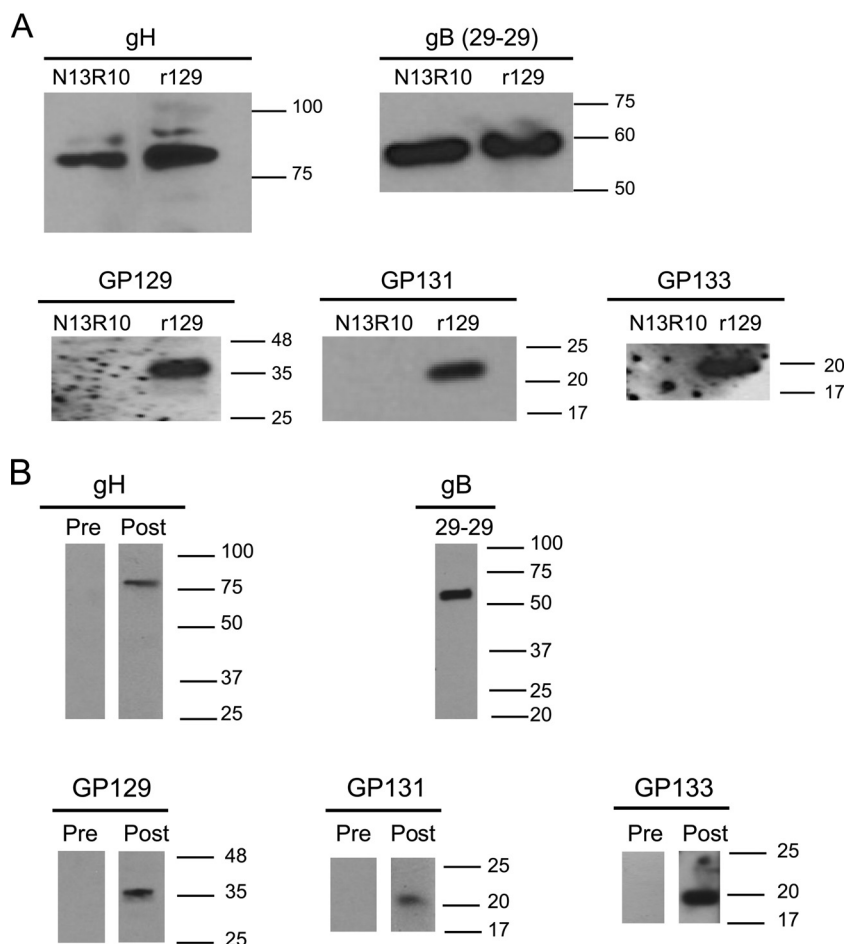
FIG 2 Virion incorporation of GP129, GP131, or GP133. (A) Virion particles were purified from supernatants of N13R10- or r129-infected GPL cultures, separated by SDS-PAGE, transferred to nitrocellulose membranes, and probed using antibodies specific for the indicated GPCMV proteins as indicated in the text. The locations of protein molecular weight standards are indicated. (B) Virion particles were purified from infected GPL monolayers inoculated with SG-adapted GPCMV (passaged once in cell culture), separated by SDS-PAGE, and probed with the indicated pre- and postimmune sera. The locations of protein molecular mass standards (kDa) are indicated.

to GPCMV gB or rabbit and guinea pig antisera specific to the gH, GP129, GP131, or GP133 proteins. While similar gB and gH levels indicated that the two virion preparations contained equivalent amounts of virions, the GP129, GP131, and GP133 proteins were present in r129 virions but undetectable in N13R10 virions (Fig. 2A). These data indicated that repair of r129 resulted in localization of the GP129, GP131, and GP133 proteins to the purified virions. As a control, the same analyses were performed on SG-derived virions, and these experiments confirmed that comparably sized proteins were produced (Fig. 2B). Preimmune sera from rabbits and guinea pigs used for generation of antibodies to PC components were not reactive to virion proteins from N13R10 or r129 virions (data not shown) or with SG virus-derived virions (Fig. 2B, preimmune). These data support the conclusion that the failure of N13R10 to express the GP129 subunit is due to the 4-bp deletion, which in turn results in failure to incorporate the GP131 or GP133 subunits into N13R10 virions. Repair of the deletion in r129 restored GP129 expression, and this in turn permitted assembly and incorporation of the full PC into r129-derived virions.

Repair of the 4-bp deletion in *GP129* and *GP130* results in enhanced virulence in immunocompromised guinea pigs. To

address whether repair of the 4-bp deletion restored pathogenic potential to BAC-derived GPCMV, a challenge study in cyclophosphamide-immunosuppressed animals was performed. Three groups of five animals were treated with cyclophosphamide on days 0 and 8 (Fig. 3). Animals were either sham inoculated s.c. with PBS or inoculated with matching 5×10^7-PFU doses of viruses N13R10 or r129. Animal weights were monitored, and blood samples were collected periodically until animals were sacrificed on day 28. All animals in the sham- and N13R10-infected groups survived the 28-day study and exhibited maximal mean weight losses of 5.6 and 6.2%, respectively (Fig. 3). In contrast, the maximal mean weight loss of r129-infected animals was 20.9% ($P <$ 0.05, compared to control or N13R10 on day 21), and two animals were sacrificed early (on days 21 and 24 postinfection) due to moribund condition after losing 24.3 and 30.2% of body weight, respectively (Fig. 3).

Mean viral loads in blood from days 3 to 21 were statistically significantly higher at each time point in the r129 group compared to the N13R10 group (Fig. 4). Animals inoculated with r129 also had a longer duration of viremia (4/5 animals positive at day 21, versus 0/5 animals in the N13R10 group at day 21). No animals
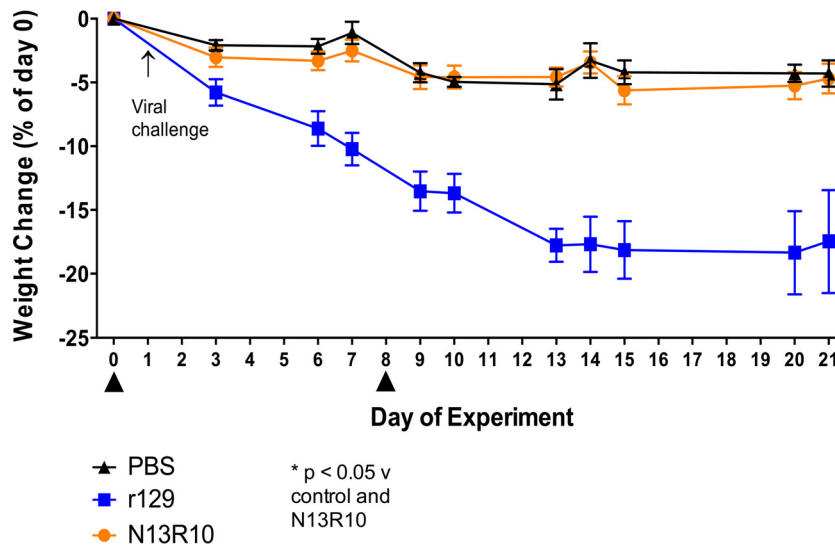
FIG 3 Weight loss following inoculation of cyclophosphamide-treated guinea pigs. Adult seronegative guinea pigs were treated with cyclophosphamide on days 0 and 8 relative to viral challenge on day 1. Groups of 5 animals were either sham inoculated s.c. with PBS or inoculated with matched 5×10^7-PFU doses of virus N13R10 or r129. Mean percentages of changes in weight $\pm$ SEM are plotted over time. Weight losses in the r129-inoculated group were significantly greater than those in the PBS- or N13R10-inoculated groups at all time points ($P < 0.05$). Arrowheads show timing of cyclophosphamide inoculation (days 0 and 8) relative to viral infection.

from the sham-inoculated (PBS) group had viral loads above the threshold of detection at any time point (data not shown).

On day 28, all surviving animals were euthanized and organs harvested for PCR-based viral load assessment. Significant differences in viral load were noted between groups (Table 1). On average, animals infected with r129 exhibited levels of viral DNA 1.1×10^6-, 1.1×10^5-, 1.5×10^6-, and 2.0×10^4-fold higher than those of N13R10-infected animals in liver, lung, spleen, and salivary gland, respectively.

Virus r129 elicits maternal viremia, congenital infection, and pup mortality in immunocompetent pregnant guinea pigs. Pregnancy/challenge studies were conducted to examine the ability of virus r129 to produce disease in pregnant guinea pigs, including maternal viremia, pup mortality, and vertical transmission. Timed-pregnant animals were divided into four groups ($n =$
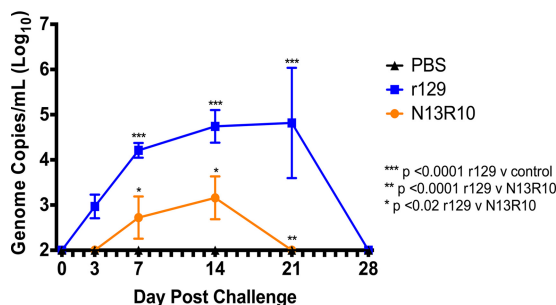

FIG 4 Systemic viral loads following inoculation of cyclophosphamide-treated guinea pigs. Viral loads were determined by qPCR of blood samples collected on days 0, 3, 7, 14, 21, and 28 from experimentally inoculated, cyclophosphamide-treated animals described in the legend to Fig. 3. The data shown are mean $\log_{10}$ genome equivalents $\pm$ SEM per milliliter of total blood. Samples with undetectable levels of DNA were assigned a value of 2 $\log_{10}$ based on the limit of PCR detection for purposes of statistical comparisons (24). *, $P < 0.02$, and **, $P < 0.0001$, r129 versus N13R10; ***, $P < 0.0001$, r129 versus control.

6 animals/group). In group 1, both GPCMV-seropositive ($n = 3$) and GPCMV-seronegative ($n = 3$) animals were challenged in the early third trimester with 1×10^5 PFU of SG-GPCMV. In groups 2 and 3, all animals were GPCMV seronegative ($n = 6$/group) and were inoculated with either 5×10^5 or 5×10^6 PFU of r129 virus, respectively. In group 4, GPCMV-seropositive ($n = 3$) and -seronegative ($n = 3$) dams were inoculated with 5×10^7 PFU of r129 virus.

Analyses of the outcomes in these groups (Table 2) demonstrated that r129 virus was capable, in a dose-dependent fashion, of producing maternal DNAemia and congenital transmission, with attendant pup mortality. In seronegative dams challenged with SG-GCMV, pup mortality was 8/12 (67%), and congenital GPCMV transmission (as gauged by any positive PCR in pup liver, lung, or spleen) occurred in 10/12 pups (83%). In seropositive dams challenged with SG-GPCMV, there was no pup mortality, but interestingly, 6/9 pups (67%) had congenital infection, although viral loads were low (Table 2). In seronegative dams ($n = 3$) challenged with r129 at the highest dose (5×10^7 PFU), pup mortality was 13/13 (100%), and congenital transmission occurred in all 13 pups (100% transmission rate). In seropositive dams challenged with this dose, mortality was 3/14 (21%), and congenital infection occurred in 7/14 pups (50%). In seronegative dams challenged with r129 at a dose of 5×10^6, pup mortality was 7/25 (28%), and transmission occurred in 24/25 pups (96%). In contrast, no pup mortality (0/20) was observed when dams were challenged with 5×10^5 PFU, although 16/20 pups (80%) nonetheless had evidence of congenital infection (Table 2).

The magnitudes of maternal DNAemia at day 7 were also similar when comparing challenge with SG-GPCMV and r129 virus. For SG-GPCMV-inoculated seronegative dams, the mean day 7 viral load was $(5.1 \pm 2.2) \times 10^6$ genomes/ml; for the r129 5×10^7-PFU seronegative group, it was $(5.5 \pm 1.5) \times 10^6$ genomes/ml; for the r129 5×10^6-PFU seronegative group, it was $(3.7 \pm 1.1) \times 10^6$ genomes/ml; and for the r129 5×10^5-PFU seronega-

TABLE 1 Tissue viral loads in cyclophosphamide-treated guinea pigs 27 days after s.c. inoculation with 5×10^7 PFU N13R10 or r129

Challenge virus	Viral load (genome copies/mg) in[a]:			
	Liver	Lung	Spleen	Salivary gland
N13R10	26 ± 11.8	16 ± 15	84.7 ± 3.7	99.4 ± 88.9
r129	$(1.3 \pm 2.5) \times 10^7$**	$(1.7 \pm 1.7) \times 10^6$*	$(1.2 \pm 1.2) \times 10^7$**	$(6.6 \pm 1.3) \times 10^5$

[a] Expressed as genome copies per milligram of tissue $\pm$ SEM. The limit of detection was ~2 genome copies/mg. For the purpose of statistical comparisons, negative samples were assigned a value of 1 copy/mg. *, $P < 0.01$ versus N13R10; **, $P < 0.001$ versus N13R10.

tive group, it was $(1.3 \pm 0.6) \times 10^6$ genomes/ml (P not significant [NS] across all seronegative dam groups, Kruskal-Wallis with Dunn's multiple comparisons).

In addition to mortality differences across groups, pup weights at birth varied in a dose-dependent fashion following inoculation of pregnant animals with SG or r129 virus (Fig. 5). Seronegative dams challenged with SG virus (1×10^5 PFU) gave birth to pups with a birth weight of 52.3 ± 6.23 g (mean $\pm$ standard error of the mean [SEM]). Seronegative dams challenged with 5×10^7 PFU of r129 virus delivered pups with a birth weight of 49.4 ± 2.69 g. These weights were significantly lower than those of pups born to seronegative dams challenged with r129 at doses of 5×10^6 PFU (85.7 ± 3.57 g) or 5×10^5 PFU (101 ± 3.9 g) (Fig. 5A). Seropositive dams challenged with SG virus gave birth to pups with a birth weight of 96.8 ± 3.96 g (mean $\pm$ SEM). Seropositive dams challenged with 5×10^7 PFU of r129 virus delivered pups with a significantly lower birth weight of 70.5 ± 5.76 g (Fig. 5B). As a control, a parallel study of healthy, noninfected dams ongoing in our vivarium during the same period produced 21 pups ($n = 7$ dams) with a birth weight of 95.7 ± 16.9 g.

Virus r129 exhibits genome stability upon serial passage in cell culture. Studies of the 22122 strain of GPCMV from ATCC demonstrated that the ATCC stock is a mixture of a full-length genome variant and a variant with a 1.6-kb deletion in the region encoding PC subunits GP129, GP131, and GP133 (10). Subsequent work suggested that even a plaque-purified full-length variant demonstrated genome instability in this region, insofar as serial passage of virus purified from a single plaque led to eventual identification of variant viruses with deletion of this 1.6-kb pathogenicity locus (18). To examine the genome stability of virus r129,

serial tissue culture passages through 11 passages were undertaken on a monthly basis by subculture on GPL cells, starting with an isolate obtained from a positive blood viral culture from an r129-challenged animal (P0). Compared to ATCC stock virus (strain 22122), which after a limited number of passages in fibroblasts demonstrated the predicted shift toward predominately the 1.6-kb deletion variant (indicated by the 348-bp PCR product), the genome of virus r129 was stable, as indicated by the exclusive presence of the 1,994-bp PCR product in Fig. 6A, upper panel. A parallel study of SG virus (maintained for >30 years exclusively *in vivo* through serial passage of SG homogenates in strain 2 guinea pigs [20]) demonstrated similar high levels of stability following serial viral passage in fibroblasts (Fig. 6A, lower panel). No evidence of the 1.6-kb deletion in either r129 or SG virus was observed after continued additional serial passage in fibroblasts out to passage 16 (data not shown).

Although PCR-based comparisons suggested at the level of gel electrophoresis that the r129 virus did not undergo deletions in the region of the viral genome previously identified as absent in a subpopulation of GPCMV variants in ATCC viral stock (10), it was noted that this level of analysis might fail to detect any mutations that included loss of the primer binding sites used to amplify the 1,994-nucleotide (nt) region. Thus, if the r129 virus had a larger deletion, including sequences on either side of the 1,994-nt region, then the PCR would potentially amplify sequence only from the small percentage of wild-type genomes present after serial passage, making viral stock appear wild-type when in fact a deletion mutant was the major form present. To address this concern, we performed additional quantitative PCR on DNA extracted from each passage (P0 to P10) of serially passaged r129

TABLE 2 Pup mortality and maternal and pup viral loads following challenge during pregnancy with SG or r129 virus

Challenge virus dose (PFU)[a]	Dams		Pups		Viral load (genome copies/mg) in[d]:		
	Dose group (n)[b]	Viral load (10^6 genome copies/ml)[c]	Infection, no. infected/total (%)	Mortality, no. of stillborn pups/total deliveries (%)	Liver	Lung	Spleen
SG virus							
1×10^5	Seronegative (3)	5.1 ± 2.2	10/12 (83)	8/12 (67)	240 ± 107	22 ± 6.4	793 ± 429
	Seropositive (3)	1.8 ± 1.8	6/9 (67)	0/9 (0)	14.3 ± 6	150 ± 88.5	32.5 ± 11.4
r129							
5×10^5	Seronegative (6)	1.3 ± 0.6	16/20 (80)	0/20 (0)	6.7 ± 1.9	47.8 ± 17.5	52.1 ± 20.1
5×10^6	Seronegative (6)	3.7 ± 1.1	24/25 (96)	7/25 (28)	117 ± 70.7	45.2 ± 14.6	212 ± 128
5×10^7	Seronegative (3)	5.5 ± 1.5	13/13 (100)	13/13 (100)	$23,129 \pm 8,820$	484 ± 196	$66,788 \pm 27,984$
	Seropositive (3)	0.7 ± 0.7	7/14 (50)	3/14 (21)	30.8 ± 25.6	51.3 ± 39.9	110 ± 76.7

[a] SG, pathogenic salivary gland extract; r129, produced in cell culture.
[b] GPCMV seronegative or seropositive.
[c] Expressed as 10^6 genome copies/ml of blood on day 7 postchallenge.
[d] Expressed as genome copies per milligram of tissue at delivery. The limit of detection was approximately 2 genome copies/mg tissue. For the purpose of statistical comparisons, negative samples were assigned a value of 1 copy/mg. For the purpose of ascertaining congenital infection rates, any pup that had qPCR values falling below the limit of detection of the assay was considered uninfected.
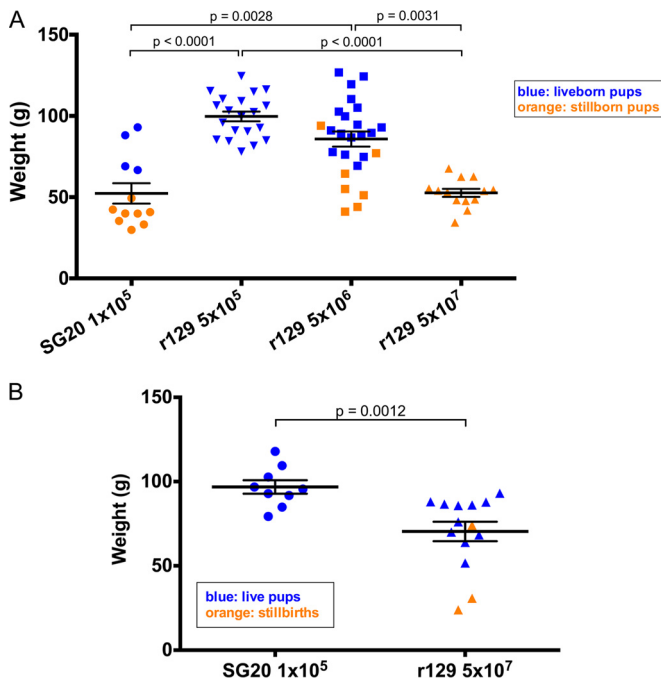
FIG 5 Pup weights following inoculation of pregnant guinea pigs with SG or r129 virus. Pregnant dams were inoculated s.c. with the indicated doses of SG or r129 virus. Pup weights and viability were determined at delivery. Data shown are for pups born to seronegative challenged dams (A) and for seropositive challenged dams (B). A dose-dependent impact on pup weights and mortality is noted with r129 virus in seronegative dams (A). Statistical comparisons were performed using Kruskal-Wallis with Dunn's multiple comparison test. Significant differences among groups are as indicated by *P* values. Blue, live-born pups; orange, stillborn pups.

virus, using both previously described primers specific for the *GP83* gene (8) and a primer-probe set spanning a 184-nt region corresponding to the *GP133* gene, a gene that would be deleted if the 1.6-kb deletion (or a larger deletion corresponding to sequences flanking this region) were selected for in cell culture. Parallel comparisons were made with serially passaged ATCC (22122) stock. Stability of this region of the genome on serial passage would be predicted to result in a ratio of *GP133* to *GP83* of ~1 by qPCR, whereas a complete deletion would result in a ratio approaching 0. This analysis demonstrated that the molar ratio of these two target sequences was ~1.0 after 10 passages in cell culture for r129 virus. In contrast, ATCC virus (22122 strain), demonstrated a decrease in the ratio of full-length to deletion variant to approximately 50% for P2 and a decrease to 18% at P3. By passage 10, the ratio of full-length to deletion variant for ATCC virus was ~6% (Fig. 6B). These results confirmed the stability of this genome region in r129 virus.

As a final confirmation of genome stability in this region, we sequenced the entire 1,994-bp PCR product, which spans all three PC ORFs contained in this region (*GP129*, *GP131*, and *GP133*) and also includes 38 bp 3′ of the *GP129* stop codon and 189 bp 5′ of the *GP133* start codon. Sequence was obtained from P0 material (obtained from a positive viral blood culture from an experimentally challenged animal) and P10 material. These sequences were identical (data not shown). An incidental amino acid substitution was noted in the GP131 ORF, H131N. Notably, this amino acid substitution fell outside the peptide region used to make the anti-GP131 antibody used for Western blot analyses.

Virus r129 exhibits end organ pathology in experimentally infected animals. To assess the ability of r129 virus to cause end organ pathology and to examine whether infection of guinea pigs with the rescued virus was associated with an alteration in host cell tropism, histological and immunohistochemical analyses of liver tissue recovered from cyclophosphamide-treated animals (inoculated with 5×10^7 PFU of N13R10 or r129 virus) were performed. In r129-inoculated animals, cytomegalic cells and inflammatory cell infiltrates were observed, and GPCMV-infected hepatocytes were detected using immunohistochemical staining for expression of GP83 or gB proteins (Fig. 7). No histopathology or positive antigen staining was detected in liver tissue harvested from animals challenged with the parental virus N13R10 (data not shown).

DISCUSSION

Viral attenuation through cell culture passage has been a valuable tool for identification of viral genes important for pathogenesis and for development of live attenuated vaccines. The first HCMV vaccine candidates were comprised of live strain Towne or AD169 viruses produced following extensive serial passage on cultured fibroblasts (26–29). When experimentally administered to human volunteers, these vaccines were highly attenuated. In contrast, 10 PFU of low-passage-number Toledo strain virus was pathogenic in humans (30). Later passages of AD169 and Toledo were found to have substantial deletions and inversions impacting a number of genes in the *UL/b′* region (31, 32). Unfortunately, these mutations cannot be clearly linked to attenuation or virulence as it is possible that some mutations occurred at latter passage and stocks that were used in humans are no longer available for study. However, analysis of the viruses in an original Towne vaccine vial revealed an ~50/50 mixture of two genome variants. The Towne-VarS genome had a large deletion of *UL/b′* sequences similar to that of AD169, while TowneVarL retained the complete complement of known HCMV ORFs (31, 33, 34). Sequencing of Towne-VarL revealed that only five annotated ORFs contain mutations that abrogate protein expression: *UL13*, *UL1*, *UL40*, *UL130*, and *US1* (35). Thus, it is reasonable to conclude that one or more of these five mutations contribute significantly to attenuation of the Towne vaccine.

Of particular interest is the mutation in *UL130*, as it disrupts formation of a functional PC. In HCMV the PC is comprised of gH, gL, UL128, UL130, and UL131A, the analogs of GPCMV gH, gL, GP129, GP131, and GP133, respectively (15–18, 25, 36). The HCMV PC is required for efficient entry into epithelial cells, endothelial cells, monocytes, and monocyte-derived dendritic cells, but UL128, UL130, and UL131A are entirely dispensable for fibroblast entry (36, 37). Thus, by rendering Towne viruses incapable of entering and replicating in these cell types, the *UL130* mutation may contribute significantly to attenuation of the Towne vaccine *in vivo*.

Live attenuated vaccines have been studied in the guinea pig model. Like Towne, GPCMV strain variants used as vaccines in early studies were attenuated by serial passage in fibroblasts (38), although the precise details of genomic deletions or mutations were not explored. Later work showed that, like HCMV, fibroblast passage of GPCMV results in mutations that remove or disrupt GPCMV genes that encode PC subunits GP129, GP131, or GP133 (16–18). In order to develop a genetic system to study GPCMV, we constructed N13R10, a full-length BAC clone of the GPCMV genome derived from a fibroblast-adapted stock (9). Virus derived from N13R10 was highly attenuated in animals compared to virulent SG-
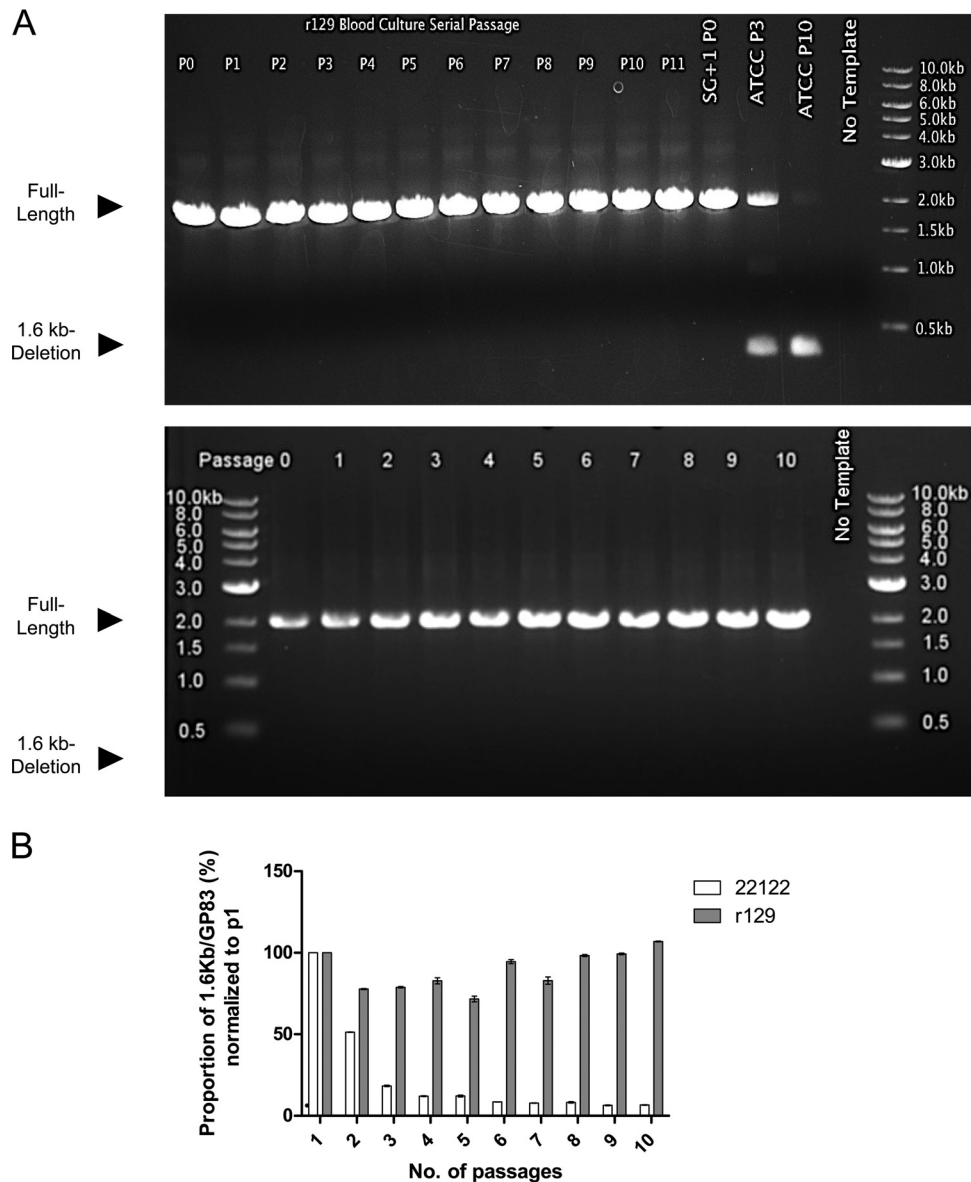
FIG 6 Stability of GPCMV genome of r129 virus following fibroblast tissue culture passage. (A) PCR was performed to evaluate for emergence of an ~1.6-kb deletion in the GPCMV genome following serial passage of r129 virus in GPL cells. (Upper panel) Virus isolated from blood culture of a cyclophosphamide-treated r129-challenged guinea pig (P0) was subjected to 11 rounds of serial passage in GPL fibroblasts (P1 to P11; P0 represents DNA purified directly from index blood culture). DNA was purified following each round of passage and subjected to PCR using primers originally described by Nozawa et al. (15). As controls, DNA was analyzed from ATCC-derived GPCMV (passaged in parallel [data shown for P3 and P10]) and SG-passaged viral stock (SG + 1/P0). (Lower panel) PCR following 10 serial passages of highly SG-adapted virus. Full-length genome was exclusively found in SG-passaged virus. Positions of molecular size markers are indicated. Arrowheads indicate positions of full-length and deletion genome variants. (B) Ratio of qPCR products following serial passage of 22122 (ATCC) and r129 virus. Primers specific for the *GP83* gene and a primer-probe set spanning a 184-bp region corresponding to the *GP133* gene (mapping to the 1.6-kb-deletion region) were used to amplify DNA extracted from each serial cell culture passage. Complete stability of the region of the genome would be predicted to result in a ratio of *GP133* to *GP83* of ~1 on serial passage, whereas selection of a deletion variant would result in a ratio approaching 0. This analysis demonstrated that the molar ratio of these two target sequences (normalized to P1) was ~1.0 after 10 passages in cell culture for r129 virus (gray bars), but that ATCC virus (22122 strain) virus demonstrated a decrease of the ratio of full-length to deletion variant to approximately 50% for P2, a decrease to 18% at P3, and a decrease to <10% for later passages (white bars).

passaged virus stocks (11, 12). To test for genetic differences that might contribute to attenuation of N13R10 virus, we sequenced the N13R10 BAC (14) and also sequenced the SG-derived GPCMV genome using DNA purified directly from salivary gland homogenates, without any intermediate passage in fibroblasts (20). Remarkably, we found only 13 differences, and of these, only 2 impacted annotated

ORFs: a 4-bp deletion/frameshift disrupting *GP129* and *GP130* and a predicted F81C amino acid substitution in GP130 that is 3′ of the 4-bp deletion/frameshift.

The present study confirms that the 4-bp deletion/frameshift is a major contributor to attenuation of N13R10. In immunocompromised animals, r129 virus induced a longer duration and
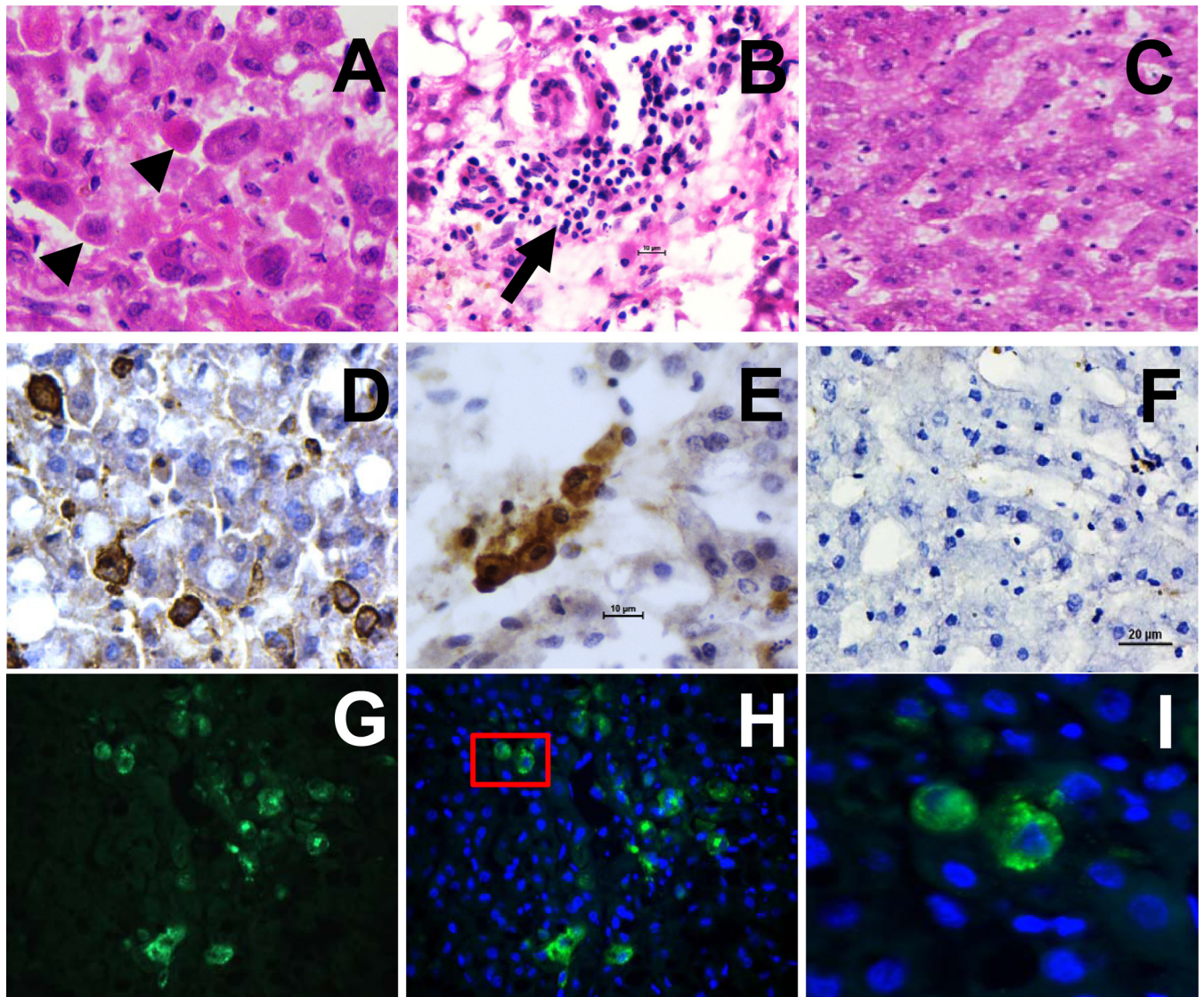
FIG 7 End organ pathology and replication with r129 virus in guinea pigs. Animals were either infected with r129 virus (A, B, D, E, G, and I) or mock infected (C and F) as described in Materials and Methods. Cytomegalic cells are noted (A [arrowheads]) as well as inflammatory cell infiltrates (B [arrow]). Both panels, ×600 magnification. Immunoperoxidase staining with GP83-specific rabbit monoclonal antibody demonstrates viral antigen in r129-infected guinea pig hepatic tissue (D and E) but not the mock-infected control (F). Immunofluorescence staining with mouse anti-guinea pig gB 29.29 monoclonal antibody (G) and DAPI counterstain (H and higher-magnification inset in panel I) confirmed GPCMV infection of hepatocytes. CMV antigen-positive cells were detected dispersed through the tissue from animals infected with r129 virus but not in uninfected or N13R10-infected controls.

higher magnitude of viremia (Fig. 4) and also produced substantially higher end organ viral loads (Table 1). Notably, r129-infected animals also experienced profound weight loss (of sufficient severity in two animals to necessitate euthanasia), while the weight changes of N13R10-infected animals were no different from those of the PBS-inoculated controls.

In the congenital infection model virus r129 was capable of establishing maternal DNAemia and inducing pup infection and mortality (Table 2). A dose response was evident with respect to the magnitude of maternal DNAemia at day 7 postinoculation, with 77% and 34% lower levels in the magnitude of viral load in the 5×10^5- and 5×10^6-PFU challenge groups, respectively, compared to the 5×10^7 challenge group. Striking differences in pup mortality were observed, with mortality rates of 100% (13/

13), 28% (7/25), and 0% (0/20) across these three doses. These differences suggest that even small variations in the magnitude of maternal DNAemia can produce differences in pup mortality. Future experiments will be required to define the threshold of maternal DNAemia associated with pup mortality using the r129 virus. There was also a clear dose response with respect to pup weights (Fig. 5A), with statistically significantly higher pup weights in the 5×10^5-PFU ($P \leq 0.0001$) and 5×10^6-PFU ($P \leq 0.004$) r129 challenge groups compared to the 5×10^7-PFU challenge group in GPCMV-seronegative dams.

From the data presented, however, attenuation of N13R10 cannot be rigorously attributed to loss of GP129 expression. The 4-bp deletion also introduces an in-frame stop after codon 5 of *GP130*, and repair of the mutation restores the normal reading

frames of both *GP129* and *GP130*. Thus, attenuation could be due to loss of GP129, loss of GP130, or cumulative effects of losing both. One limitation of these studies is that both the N13R10 and r129 viruses contain missense mutations in GP130. The missense mutation in N13R10 is irrelevant, as in N13R10 it is 3′ of the frameshift, and in r129 it was successfully repaired. However, during BAC genetic manipulation, additional mutations occurred in *GP130*. Consequently, while correction of the frameshift in r129 is predicted to restore expression of a fully wild-type GP129 protein, the predicted GP130 protein contains two amino acid substitutions, R93Q and P97S. It should be noted, however, that there is no evidence to date to indicate that *GP130* encodes a functional protein. The predicted 15-kDa 130-amino-acid protein has no homology to any known or predicted proteins in the database. Although an unspliced *GP130*-specific transcript was detected in infected cells by reverse transcriptase PCR in previous studies, no transcript has been noted by Northern blotting ([17]). While the *GP130* ORF is conserved in the related CIDMTR strain of GPCMV ([39]), the amino acid homology between predicted GP130 proteins is limited to the region of overlap with *GP129* on the negative strand, but is highly divergent between the two strains downstream of codon Pro_{80}, suggesting that partial conservation of *GP130* likely derives from selective pressure directed against *GP129*. Another substitution was noted in a flanking ORF, insofar as sequence analyses of a 1,994-nt region (spanning the region from *GP129* to *GP133*) following 1 round of passage in guinea pigs and >10 rounds of passage in cell culture identified one additional incidental amino acid substitution (H131N) in GP131. The 1,994-bp region was otherwise highly stable, and identical sequence in this region was noted following >10 rounds of virus passage in cell culture. Further experiments will be required to evaluate whether a bona fide GP130 protein exists in GPCMV-infected cells and to investigate any potential role for *GP130* and *GP131* missense mutations in the pathogenesis of r129 virus. Additional analyses will also be required to ensure that other point mutations and/or small deletions are not present in other regions of the r129 viral genome. The recent isolation of viral mutants that selectively disrupt *GP129* or *GP130* (without impacting the other [unpublished data]) should serve to firmly establish the relative contributions of each ORF to viral pathogenesis.

While the composition of the GPCMV PC is similar to that of the HCMV PC, it is not yet clear that it serves an equivalent function. Progress toward characterizing the role of the GPCMV PC in epithelial or endothelial tropism has been frustrated by a lack of established guinea pig epithelial or endothelial cell lines that support GPCMV replication. Using primary cells, Yamada et al. found that the GPCMV PC is required for infection of monocytes and macrophages ([16]), which is consistent with data that HCMV infection of monocytes is PC dependent ([40]). However, using primary endothelial cells, Auerbach et al. did not observe an endothelial cell-specific defect for a PC-negative mutant virus, but rather found that deletion of PC subunit genes caused an equivalent reduction in entry efficiency for both endothelial and fibroblast cells ([18]). Thus, although further studies are needed, current evidence suggests that GPCMV and HCMV PCs may have distinct as well as overlapping functions.

While repair of the frameshift mutation in the *GP129-GP130* locus greatly enhanced the virulence of r129 compared to N13R10, r129 was still less virulent than SG virus. An ~15-fold-higher challenge dose of r129 (5×10^6 PFU) was needed to match

levels of transmission, pup mortality, or pup viral loads elicited by the standard pathogenic SG virus challenge (1×10^5 PFU). Remaining genetic differences could contribute to this reduced virulence. As noted above, r129 encodes a hypothetical GP130 protein containing two amino acid substitutions and a GP131 protein with a single amino acid change, and while the other 11 sequence differences noted upon comparison of N13R10 and SG virus do not lie within currently annotated ORFs, some could impact unannotated ORFs that encode authentic proteins, while others might impact regulatory sequences or influence posttranscriptional events such as splicing or mRNA stability. In addition, excision of the BAC origin leaves a residual 35-bp loxP site in r129 that disrupts an unannotated ORF that encodes a 136-amino-acid hypothetical protein that has no homology to any known or predicted proteins in the database. It is possible that disruption of this ORF contributes to reduced virulence of r129 relative to SG virus.

It is also likely that epigenetic factors unique to SG virus (produced in salivary gland) and absent from r129 virus (produced in cell culture) account, at least in part, for the greater virulence of SG virus, although the precise biological basis for this effect is poorly understood. This hypothesis is supported by observations that attenuation of murine cytomegalovirus (MCMV) occurs within one passage in cell culture but is reversed by one passage *in vivo* ([41]). Thus, it is possible that the protein compositions and consequently the tropisms of virions produced in salivary gland epithelial cells *in vivo* may differ from those produced in cultured fibroblasts. Another study suggested that the increased virulence of MCMV SG virus *in vivo* might be related to the fact that SG virus is produced in epithelial cells, whereas virus generated in other compartments in the infected mouse, including visceral organs, may predominantly be produced following replication in fibroblasts ([42]). Other studies have suggested that the fact that T cell immunity is limited in the salivary gland allows CMV to exploit the mucosal microenvironment to replicate more effectively ([43]). Evidence from HCMV suggests that viruses produced in different cell types can differ in their phenotypes, supporting this hypothesis ([44], [45]). Further studies will be required to elucidate the mechanism(s) responsible for the increased virulence of SG-passaged GPCMV.

Notably, we observed a high degree of genome stability of the r129 virus, compared to the ATCC (22122) strain. Serial tissue culture passage through 11 passages, starting with an isolate from a positive blood viral culture from an r129-challenged animal (P0), indicated no evidence of the deletion of the 1.6-kb region that was observed in a subpopulation of GPCMV variants that was identified in studies of the ATCC strain by PCR analysis ([10]). Compared to ATCC stock virus, which after a limited number of passages in fibroblasts demonstrated the predicted shift toward predominately the 1.6-kb-deletion variant (indicated by the 348-nt PCR product in [Fig. 6A]), PCR of the genome of virus r129 indicated the exclusive presence of the 1,994-nt PCR product corresponding to a full-length, wild-type genome configuration ([Fig. 6A]). To exclude the possibility of an adventitious deletion upstream of the primers used for PCR, a qPCR comparison of the relative ratio of *GP83* (an essential gene) signal to *GP133* signal was performed. This indicated a stable ratio for r129 virus but the predicted decrease in the ratio of *GP83* to *GP133* signal in serially passaged virus ([Fig. 6B]).

Although r129 virus is not as virulent as SG virus, it is important to note that a 5×10^6-PFU challenge with r129 viral stock

produced in cell culture is sufficient to elicit transmission and fetal disease similar to the standard SG challenge dose used in this model. As r129 culture supernatants can reach 10^8 PFU/ml, routine challenge with 5×10^6 PFU is readily achievable. The r129 virus was also demonstrated to produce immunohistochemically demonstrable infection of epithelial cells (hepatocytes) in challenged animals (Fig. 7). It was of further interest that reinfection of immune dams was able, in some instances, to lead to transplacental transmission, fetal infection, and fetal loss. Importantly, because cell culture-produced r129 is pathogenic and is derived from a BAC clone that can be genetically manipulated in *E. coli*, the N13R10-r129 BAC provides a platform to explore the genetic basis of viral pathogenesis in this important animal model of congenital infection.

Finally, extension of these observations in GPCMV to HCMV may shed light on understanding the mechanism(s) of attenuation of Towne vaccine. By analogy with the impact of the *GP129* mutation on GPCMV virulence, it seems likely that the mutation in *UL130* contributes significantly to the safety of the Towne vaccine. It is ironic that the same mutation may also diminish the vaccine's efficacy. People who are naturally infected with wild-type strains of HCMV develop robust epithelial cell-specific neutralizing responses that are largely mediated by antibodies directed against the PC (46–52). Towne vaccination fails to induce comparable epithelial cell neutralizing activities, presumably because the *UL130* mutation in the Towne strain prevents the assembly of functional PCs *in vivo* (46, 53). A whole-virus, replication-defective vaccine has been developed by Merck and is currently undergoing phase 1 testing (https://clinicaltrials.gov/ct2/show /NCT01986010?term=merck+cytomegalovirus&rank=1). This vaccine incorporates genetic modifications that allow conditional replication in cell culture but block replication *in vivo*. Unlike Towne, this virus expresses a functional PC, and despite the inability to replicate, elicits robust epithelial cell-specific neutralizing responses in animals (50). While it is not yet known whether the GPCMV PC contains analogous neutralizing epitopes, the r129 virus nevertheless provides a platform with which to evaluate the role of the PC in vaccine efficacy. Further, the PC-positive r129 virus can be used in the animal model to emulate replication-defective strategies similar to those employed by Merck or, as we have pursued, live vaccines that are rationally attenuated through deletion of viral immune evasion functions (11, 24). Future studies based on r129 promise to advance the guinea pig model and make important contributions to our understanding of cytomega-loviral pathogenesis and vaccine efficacy.

ACKNOWLEDGMENTS

FUNDING INFORMATION

REFERENCES

1. **Arvin AM, Fast P, Myers M, Plotkin S, Rabinovich R.** 2004. Vaccine development to prevent cytomegalovirus disease: report from the National Vaccine Advisory Committee. Clin Infect Dis **39:**233–239. http://dx .doi.org/10.1086/421999.

2. **Plotkin S.** 2015. The history of vaccination against cytomegalovirus. Med Microbiol Immunol **204:**247–254. http://dx.doi.org/10.1007/s00430-015 -0388-z.

3. **Schleiss MR.** 2013. Developing a vaccine against congenital cytomegalovirus (CMV) infection: what have we learned from animal models? Where should we go next? Future Virol **8:**1161–1182. http://dx.doi.org/10.2217/fvl.13.106.

4. **Dogra P, Sparer TE.** 2014. What we have learned from animal models of HCMV. Methods Mol Biol **1119:**267–288. http://dx.doi.org/10.1007/978 -1-62703-788-4_15.

5. **Schleiss MR, McVoy MA.** 2010. Guinea pig cytomegalovirus (GPCMV): a model for the study of the prevention and treatment of maternal-fetal transmission. Future Virol **5:**207–217. http://dx.doi.org/10.2217/fvl.10.8.

6. **Bravo FJ, Bernstein DI, Beadle JR, Hostetler KY, Cardin RD.** 2011. Oral hexadecyloxypropyl-cidofovir therapy in pregnant guinea pigs improves outcome in the congenital model of cytomegalovirus infection. Antimicrob Agents Chemother **55:**35–41. http://dx.doi.org/10 .1128/AAC.00971-10.

7. **Auerbach MR, Yan D, Vij R, Hongo JA, Nakamura G, Vernes JM, Meng YG, Lein S, Chan P, Ross J, Carano R, Deng R, Lewin-Koh N, Xu M, Feierbach B.** 2014. A neutralizing anti-gH/gL monoclonal antibody is protective in the guinea pig model of congenital CMV infection. PLoS Pathog **10:**e1004060. http://dx.doi.org/10.1371/journal.ppat.1004060.

8. **Schleiss MR, Choi KY, Anderson J, Mash JG, Wettendorff M, Mossman S, Van Damme M.** 2014. Glycoprotein B (gB) vaccines adjuvanted with AS01 or AS02 protect female guinea pigs against cytomegalovirus (CMV) viremia and offspring mortality in a CMV-challenge model. Vaccine **32:** 2756–2762. http://dx.doi.org/10.1016/j.vaccine.2013.07.010.

9. **Cui X, McGregor A, Schleiss MR, McVoy MA.** 2008. Cloning the complete guinea pig cytomegalovirus genome as an infectious bacterial artificial chromosome with excisable origin of replication. J Virol Methods **149:**231–239. http://dx.doi.org/10.1016/j.jviromet.2008.01.031.

10. **Nozawa N, Yamamoto Y, Fukui Y, Katano H, Tsutsui Y, Sato Y, Yamada S, Inami Y, Nakamura K, Yokoi M, Kurane I, Inoue N.** 2008. Identification of a 1.6 kb genome locus of guinea pig cytomegalovirus required for efficient viral growth in animals but not in cell culture. Virology **379:**45–54. http://dx.doi.org/10.1016/j.virol.2008.06.018.

11. **Crumpler MM, Choi KY, McVoy MA, Schleiss MR.** 2009. A live guinea pig cytomegalovirus vaccine deleted of three putative immune evasion genes is highly attenuated but remains immunogenic in a vaccine/ challenge model of congenital cytomegalovirus infection. Vaccine **27:** 4209–4218. http://dx.doi.org/10.1016/j.vaccine.2009.04.036.

12. **Olejniczak MJ, Choi KY, McVoy MA, Cui X, Schleiss MR.** 2011. Intravaginal cytomegalovirus (CMV) challenge elicits maternal viremia and results in congenital transmission in a guinea pig model. Virol J **8:**89. http://dx.doi.org/10.1186/1743-422X-8-89.

13. **Bratcher DF, Bourne N, Bravo FJ, Schleiss MR, Slaoui M, Myers MG, Bernstein DI.** 1995. Effect of passive antibody on congenital cytomegalovirus infection in guinea pigs. J Infect Dis **172:**944–950. http://dx.doi.org /10.1093/infdis/172.4.944.

14. **Yang D, Alam Z, Cui X, Chen M, Sherrod CJ, McVoy MA, Schleiss MR, Dittmer DP.** 2014. Complete genome sequence of cell culture-attenuated guinea pig cytomegalovirus cloned as an infectious bacterial artificial chromosome. Genome Announc **2:**e00928-14. http://dx.doi.org/10.1128 /genomeA.00928-14.

15. **Gnanandarajah JS, Gillis PA, Hernandez-Alvarado N, Higgins L, Markowski TW, Sung H, Lumley S, Schleiss MR.** 2014. Identification by mass spectrometry and immune response analysis of guinea pig cytomegalovirus (GPCMV) pentameric complex proteins GP129, 131 and 133. Viruses **6:**727–751. http://dx.doi.org/10.3390/v6020727.

16. **Yamada S, Fukuchi S, Hashimoto K, Fukui Y, Tsuda M, Kataoka M, Katano H, Inoue N.** 2014. Guinea pig cytomegalovirus GP129/131/133, homologues of human cytomegalovirus UL128/130/131A, are necessary for infection of monocytes and macrophages. J Gen Virol **95:**1376–1382. http://dx.doi.org/10.1099/vir.0.064527-0.

17. **Yamada S, Nozawa N, Katano H, Fukui Y, Tsuda M, Tsutsui Y, Kurane I, Inoue N.** 2009. Characterization of the guinea pig cytomegalovirus genome locus that encodes homologs of human cytomegalovirus major immediate-early genes, UL128, and UL130. Virology **391:**99–106. http: //dx.doi.org/10.1016/j.virol.2009.05.034.

18. **Auerbach M, Yan D, Fouts A, Xu M, Estevez A, Austin CD, Bazan F, Feierbach B.** 2013. Characterization of the guinea pig CMV gH/gL/ GP129/GP131/GP133 complex in infection and spread. Virology **441:**75– 84. http://dx.doi.org/10.1016/j.virol.2013.03.008.

19. **Warming S, Costantino N, Court DL, Jenkins NA, Copeland NG.** 2005. Simple and highly efficient BAC recombineering using galK selection. Nucleic Acids Res **33:**e36. http://dx.doi.org/10.1093/nar/gni035.

20. **Yang D, Tamburro K, Dittmer D, Cui X, McVoy MA, Hernandez-Alvarado N, Schleiss MR.** 2013. Complete genome sequence of pathogenic guinea pig cytomegalovirus from salivary gland homogenates of infected animals. Genome Announc **1:**e0005413. http://dx.doi.org/10.1128/genomeA.00054-13.

21. **Cui X, McGregor A, Schleiss MR, McVoy MA.** 2009. The impact of genome length on replication and genome stability of the herpesvirus guinea pig cytomegalovirus. Virology **386:**132–138. http://dx.doi.org/10.1016/j.virol.2008.12.030.

22. **Schleiss MR, Bourne N, Stroup G, Bravo FJ, Jensen NJ, Bernstein DI.** 2004. Protection against congenital cytomegalovirus infection and disease in guinea pigs, conferred by a purified recombinant glycoprotein B vaccine. J Infect Dis **189:**1374–1381. http://dx.doi.org/10.1086/382751.

23. **Schleiss MR, Bernstein DI, McVoy MA, Stroup G, Bravo F, Creasy B, McGregor A, Henninger K, Hallenberger S.** 2005. The non-nucleoside antiviral, BAY 38-4766, protects against cytomegalovirus (CMV) disease and mortality in immunocompromised guinea pigs. Antiviral Res **65:**35–43. http://dx.doi.org/10.1016/j.antiviral.2004.09.004.

24. **Schleiss MR, Bierle CJ, Swanson EC, McVoy MA, Wang JB, Al-Mahdi Z, Geballe AP.** 2015. Vaccination with a live attenuated cytomegalovirus devoid of a protein kinase R inhibitory gene results in reduced maternal viremia and improved pregnancy outcome in a guinea pig congenital infection model. J Virol **89:**9727–9738. http://dx.doi.org/10.1128/JVI.01419-15.

25. **Ryckman BJ, Rainish BL, Chase MC, Borton JA, Nelson JA, Jarvis MA, Johnson DC.** 2008. Characterization of the human cytomegalovirus gH/gL/UL128-131 complex that mediates entry into epithelial and endothelial cells. J Virol **82:**60–70. http://dx.doi.org/10.1128/JVI.01910-07.

26. **Elek SD, Stern H.** 1974. Development of a vaccine against mental retardation caused by cytomegalovirus infection in utero. Lancet **i:**1–5.

27. **Neff BJ, Weibel RE, Buynak EB, McLean AA, Hilleman MR.** 1979. Clinical and laboratory studies of live cytomegalovirus vaccine Ad-169. Proc Soc Exp Biol Med **160:**32–37. http://dx.doi.org/10.3181/00379727-160-40382.

28. **Schleiss MR, Heineman TC.** 2005. Progress toward an elusive goal: current status of cytomegalovirus vaccines. Expert Rev Vaccines **4:**381–406. http://dx.doi.org/10.1586/14760584.4.3.381.

29. **Plotkin SA, Furukawa T, Zygraich N, Huygelen C.** 1975. Candidate cytomegalovirus strain for human vaccination. Infect Immun **12:**521–527.

30. **Plotkin SA, Starr SE, Friedman HM, Gonczol E, Weibel RE.** 1989. Protective effects of Towne cytomegalovirus vaccine against low-passage cytomegalovirus administered as a challenge. J Infect Dis **159:**860–865. http://dx.doi.org/10.1093/infdis/159.5.860.

31. **Cha TA, Tom E, Kemble GW, Duke GM, Mocarski ES, Spaete RR.** 1996. Human cytomegalovirus clinical isolates carry at least 19 genes not found in laboratory strains. J Virol **70:**78–83.

32. **Prichard MN, Penfold ME, Duke GM, Spaete RR, Kemble GW.** 2001. A review of genetic differences between limited and extensively passaged human cytomegalovirus strains. Rev Med Virol **11:**191–200. http://dx.doi.org/10.1002/rmv.315.

33. **Hahn G, Rose D, Wagner M, Rhiel S, McVoy MA.** 2003. Cloning of the genomes of human cytomegalovirus strains Toledo, TownevarRIT3, and Towne_long as BACs and site-directed mutagenesis using a PCR-based technique. Virology **307:**164–177. http://dx.doi.org/10.1016/S0042-6822(02)00061-2.

34. **Bradley AJ, Lurain NS, Ghazal P, Trivedi U, Cunningham C, Baluchova K, Gatherer D, Wilkinson GW, Dargan DJ, Davison AJ.** 2009. High-throughput sequence analysis of variants of human cytomegalovirus strains Towne and AD169. J Gen Virol **90:**2375–2380. http://dx.doi.org/10.1099/vir.0.013250-0.

35. **Cui X, Adler SP, Davison AJ, Smith L, Habib E-SE, McVoy MA.** 2012. Bacterial artificial chromosome clones of viruses comprising the Towne cytomegalovirus vaccine. J Biomed Biotechnol **2012:**428498. http://dx.doi.org/10.1155/2012/428498.

36. **Wang D, Shenk T.** 2005. Human cytomegalovirus virion protein complex required for epithelial and endothelial cell tropism. Proc Natl Acad Sci U S A **102:**18153–18158. http://dx.doi.org/10.1073/pnas.0509201102.

37. **Hahn G, Revello MG, Patrone M, Percivalle E, Campanini G, Sarasini A, Wagner M, Gallina A, Milanesi G, Koszinowski U, Baldanti F, Gerna G.** 2004. Human cytomegalovirus UL131-128 genes are indispensable for virus growth in endothelial cells and virus transfer to leukocytes. J Virol **78:**10023–10033. http://dx.doi.org/10.1128/JVI.78.18.10023-10033.2004.

38. **Bia FJ, Griffith BP, Tarsio M, Hsiung GD.** 1980. Vaccination for the prevention of maternal and fetal infection with guinea pig cytomegalovirus. J Infect Dis **142:**732–738. http://dx.doi.org/10.1093/infdis/142.5.732.

39. **Schleiss MR, McAllister S, Armien AG, Hernandez-Alvarado N, Fernandez-Alarcon C, Zabeli JC, Ramaraj T, Crow JA, McVoy MA.** 2014. Molecular and biological characterization of a new isolate of guinea pig cytomegalovirus. Viruses **6:**448–475. http://dx.doi.org/10.3390/v6020448.

40. **Straschewski S, Patrone M, Walther P, Gallina A, Mertens T, Frascaroli G.** 2011. Protein pUL128 of human cytomegalovirus is necessary for monocyte infection and blocking of migration. J Virol **85:**5150–5158. http://dx.doi.org/10.1128/JVI.02100-10.

41. **Osborn JE, Walker DL.** 1971. Virulence and attenuation of murine cytomegalovirus. Infect Immun **3:**228–236.

42. **Selgrade MK, Nedrud JG, Collier AM, Gardner DE.** 1981. Effects of cell source, mouse strain, and immunosuppressive treatment on production of virulent and attenuated murine cytomegalovirus. Infect Immun **33:**840–847.

43. **Humphreys IR, de Trez C, Kinkade A, Benedict CA, Croft M, Ware CF.** 2007. Cytomegalovirus exploits IL-10-mediated immune regulation in the salivary glands. J Exp Med **204:**1217–1225. http://dx.doi.org/10.1084/jem.20062424.

44. **Scrivano L, Sinzger C, Nitschko H, Koszinowski UH, Adler B.** 2011. HCMV spread and cell tropism are determined by distinct virus populations. PLoS Pathog **7:**e1001256. http://dx.doi.org/10.1371/journal.ppat.1001256.

45. **Wang D, Yu QC, Schröer J, Murphy E, Shenk T.** 2007. Human cytomegalovirus uses two distinct pathways to enter retinal pigmented epithelial cells. Proc Natl Acad Sci U S A **104:**20037–20042. http://dx.doi.org/10.1073/pnas.0709704104.

46. **Cui X, Meza BP, Adler SP, McVoy MA.** 2008. Cytomegalovirus vaccines fail to induce epithelial entry neutralizing antibodies comparable to natural infection. Vaccine **26:**5760–5766. http://dx.doi.org/10.1016/j.vaccine.2008.07.092.

47. **Gerna G, Sarasini A, Patrone M, Percivalle E, Fiorina L, Campanini G, Gallina A, Baldanti F, Revello MG.** 2008. Human cytomegalovirus serum neutralizing antibodies block virus infection of endothelial/epithelial cells, but not fibroblasts, early during primary infection. J Gen Virol **89:**853–865. http://dx.doi.org/10.1099/vir.0.83523-0.

48. **Fouts AE, Chan P, Stephan JP, Vandlen R, Feierbach B.** 2012. Antibodies against the gH/gL/UL128/UL130/UL131 complex comprise the majority of the anti-cytomegalovirus (anti-CMV) neutralizing antibody response in CMV hyperimmune globulin. J Virol **86:**7444–7447. http://dx.doi.org/10.1128/JVI.00467-12.

49. **Macagno A, Bernasconi NL, Vanzetta F, Dander E, Sarasini A, Revello MG, Gerna G, Sallusto F, Lanzavecchia A.** 2010. Isolation of human monoclonal antibodies that potently neutralize human cytomegalovirus infection by targeting different epitopes on the gH/gL/UL128-131A complex. J Virol **84:**1005–1013. http://dx.doi.org/10.1128/JVI.01809-09.

50. **Freed DC, Tang Q, Tang A, Li F, He X, Huang Z, Meng W, Xia L, Finnefrock AC, Durr E, Espeseth AS, Casimiro DR, Zhang N, Shiver JW, Wang D, An Z, Fu TM.** 2013. Pentameric complex of viral glycoprotein H is the primary target for potent neutralization by a human cytomegalovirus vaccine. Proc Natl Acad Sci U S A **110:**E4997–E5005. http://dx.doi.org/10.1073/pnas.1316517110.

51. **Lilleri D, Kabanova A, Lanzavecchia A, Gerna G.** 2012. Antibodies against neutralization epitopes of human cytomegalovirus gH/gL/pUL128-130-131 complex and virus spreading may correlate with virus control in vivo. J Clin Immunol **32:**1324–1331. http://dx.doi.org/10.1007/s10875-012-9739-3.

52. **Lilleri D, Kabanova A, Revello MG, Percivalle E, Sarasini A, Genini E, Sallusto F, Lanzavecchia A, Corti D, Gerna G.** 2013. Fetal human cytomegalovirus transmission correlates with delayed maternal antibodies to gH/gL/pUL128-130-131 complex during primary infection. PLoS One **8:**e59863. http://dx.doi.org/10.1371/journal.pone.0059863.

53. **Patrone M, Secchi M, Fiorina L, Ierardi M, Milanesi G, Gallina A.** 2005. Human cytomegalovirus UL130 protein promotes endothelial cell infection through a producer cell modification of the virion. J Virol **79:**8361–8373. http://dx.doi.org/10.1128/JVI.79.13.8361-8373.2005.